2013

Magnetic phases of cobalt atomic clusters on tungsten

Pavel V. Lukashev
University of Nebraska–Lincoln, pavel.lukashev@uni.edu

Ji-Hyun Kim
Sookmyung Womens University, Seoul

Seolum Yang
Sookmyung Womens University, Seoul

Jae-Sung Kim
Sookmyung Womens University, Seoul

Xumin Chen
University of Nebraska–Lincoln

See next page for additional authors

Published in *Journal of Physics: Condensed Matter* 25:3 (2013), 036003 (4 pp.)
doi: 10.1088/0953-8984/25/3/036003

Submitted September 21, 2012; revised November 26, 2012; published online December 10, 2012.

Magnetic phases of cobalt atomic clusters on tungsten

Pavel V. Lukashev,[1] Ji-Hyun Kim,[2] Seolun Yang,[2] Jae-Sung Kim,[2] Xumin Chen,[1] Geoffrey Rojas,[1] Jan Honolka,[3] Ralph Skomski,[1] Axel Enders,[1] and Renat F. Sabirianov [4]

1. Department of Physics and Astronomy and Nebraska Center for Materials and Nanoscience, University of Nebraska–Lincoln, Lincoln, NE 68588, USA
2. Department of Physics, Sookmyung Womens University, Seoul, 140-741, South Korea
3. Max Planck Institute for Solid State Physics, Heisenbergstr. 1, Stuttgart, D-70569, Germany
4. Department of Physics, University of Nebraska at Omaha, Omaha, NE 68182, USA

Corresponding author —P. V. Lukashev, pavel.lukashev@unl.edu

Abstract
First-principle calculations are employed to show that the magnetic structure of small atomic clusters of Co, formed on a crystalline W(110) surface and containing 3–12 atoms, strongly deviates from the usual stable ferromagnetism of Co in other systems. The clusters are ferri-, ferro- or non-magnetic, depending on cluster size and geometry. We determine the atomic Co moments and their relative alignment, and show that antiferromagnetic spin alignment in the Co clusters is caused by hybridization with the tungsten substrate and band filling. This is in contrast with the typical strong ferromagnetism of bulk Co alloys, and ferromagnetic coupling in Fe/W(110) clusters.

Magnetic nanostructures often exhibit spin configurations that do not naturally occur in bulk materials. For example, iron is a prototypical ferromagnet in its bulk *bcc* phase but exhibits low-spin–high-spin transitions, antiferromagnetism, complex spin structures and even non-collinear magnetic order in thin films and other nanostructures [1–5]. This diversity is especially pronounced for dense-packed *fcc*-like atomic environments [6–8]. By contrast, metallic cobalt tends to exhibit stable ferromagnetism (FM), even in dense-packed atomic arrangements [9] and in nanostructures [10].

The magnetic moment and its average, the magnetization, are the most fundamental magnetic properties. They depend on the atomic environment and can be tuned by alloying and nanostructuring, thereby creating [11], enhancing [12] or reducing [13] the magnetization and yielding phenomena such as high-spin–low-spin transitions [2]. The coupling between magnetic moments is antiferromagnetic (AFM) in a number of materials, especially if the structures contain atoms from the middle of the transition metals series, such as Cr, Mn and Fe. Recent examples of magnetic order that show characteristic properties as a result of nanostructuring are the complex magnetic ground state in Fe monolayers on Ir(111) [14], antiferromagnetism in Fe layers on W(100) [3], and the non-collinear spin alignment in Mn on W(110) [5]. Electronic hybridization with the substrate often plays an important role, adding complexity to effects such as the non-collinear spin alignment in Cr trimers as a result of geometric frustration of AFM interactions [15].

The frequent occurrence of non-ferromagnetic spin configurations in Cr, Mn, and to a lesser extent in Fe is caused by the general trend towards AFM interactions in metals with nearly half-filled d-bands. By contrast, late iron-series transition-metal elements, especially Co, tend to exhibit robust ferromagnetism in strained systems, nanostructures, and alloys. A good example of the latter is the hexagonal intermetallic Y_2Co_{17}, which maintains a high Curie temperature T_C = 894 °C, as compared to T_C = 44 °C in the isostructural alloy Y_2Fe_{17} [9]. Cobalt-poor alloys with non-magnetic metals such as W and Y tend to lose their magnetic moments but become non-magnetic rather than

ferrimagnetic or AFM [16]. However, the monolayer of Co on W(001) surface was surprisingly predicted to have antiferromagnetic ground state [17].

In the present work, we demonstrate from first principles that atomic cobalt clusters of particular size and geometry on the W(110) surface may exhibit AFM coupling, not present in layers of Co on W(110) [18–20] and on 2D tungsten carbide layers [21], and especially in striking contrast to the FM coupling in bulk Co, ultrathin films and nanoclusters of Co on various *fcc* and *bcc* substrates [10]. For comparison, we also show that such a behavior is absent in the Fe clusters of the similar geometry.

Figure 1(a) shows the structural model used for the calculations. We consider Co_N atomic clusters containing N = 3–12 Co atoms on *bcc*(110) tungsten supercell. We perform our calculations using the projector augmented wave (PAW) method [22], implementation of PAW in Vienna *ab initio* simulation package (VASP) [23] within Perdew–Burke–Ernzerhof (PBE) generalized gradient approximation (GGA) [24] of the density functional theory (DFT). The simulations were performed using periodic boundary conditions in the 3 layer slab geometry. In particular, the unit cell for Co_4 clusters has lattice parameters a = 8.94 Å, b = 6.32 Å, c = 20 Å (this corresponds to 2 by 2 translations of W(110) unit cell), with vacuum layer of ~12 Å in c-direction. The unit cell for all other clusters has lattice parameters a = 8.94 Å, b = 12.64 Å, c = 20 Å. We use 6 × 6 × 1 k-point sampling for smaller and 4 × 4 × 1 k-point sampling for larger cells, and the Blöchl's tetrahedron integration method [25]. We relax the atomic positions of all atoms in the unit cells until Hellmann–Feynman forces were less than 0.005 eV Å^{-1}. Based on the relaxed positions, we use second-order perturbation theory and the Green's function approach [7, 26] to calculate the exchange interaction parameters. The effective exchange interaction is calculated from

$$J_0 = \frac{1}{4\pi}\sum_{LL'} \mathrm{Im}\int_{-\infty}^{E_F} \{\Delta_l^0 (T_{LL'}^{00\uparrow} - T_{LL'}^{00\downarrow}) + \Delta_l^0 T_{LL'}^{00\uparrow} + \Delta_l^0 T_{LL'}^{00\downarrow}\}\, \mathrm{d}E$$

where $\Delta = t_{0\uparrow}^{-1} - t_{0\downarrow}^{-1}$, and t^{-1} is the inverse single-site scattering matrix and T is the matrix of the scattering-path operator.

Figure 1(b) summarizes the calculated results for the net magnetic moments $\langle m \rangle$ of Co and Fe clusters as a function of the number N of atoms per cluster. The magnetization of the rhombic Co_4 and Co_{12} clusters is strongly reduced by AFM exchange inside the clusters. In all clusters, the spin density is localized at the Co atoms but slightly extended towards the nearest W neighbors. This indicates the hybridization of Co and W states, which, however, does not yield a significant spin polarization in the W substrate. The present calculations indicate the AFM exchange in the system, although the sign and strength of the exchange coupling vary with cluster configuration, and we also obtain FM (Co_3, Co_5) and non-magnetic (rhomboidal Co_4, Co_6, Co_8) spin structures. Most striking is the transition from ferrimagnetic Co_4 to non-magnetic Co_6, where the atomic arrangement with respect to the substrate is similar, and the different behavior of the rhombic and parallelogram Co_4 clusters (see Figure 1(a)).

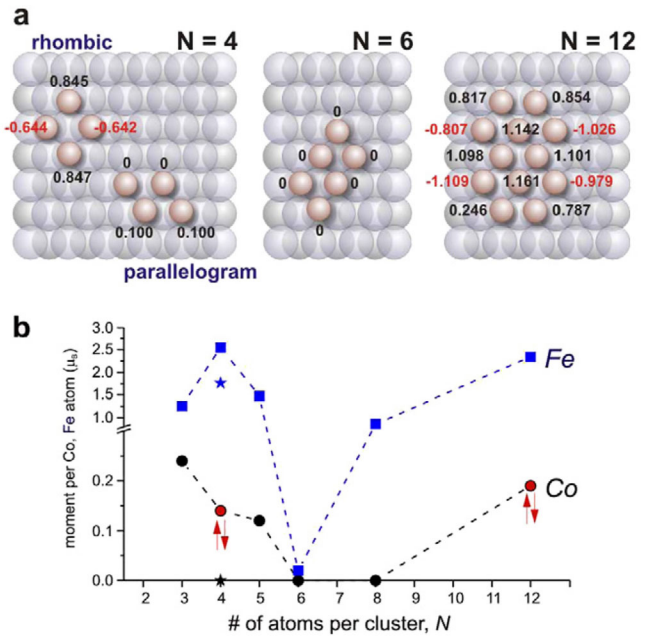

Figure 1. Structure and magnetism of Co and Fe clusters on W(110): (a) Assumed arrangement of the atoms in clusters Co_4, Co_6 and Co_{12}, with calculated moments for each atom. Moments labeled in black and red correspond to spins pointing into and out of the surface plane, respectively. (b) Calculated magnetic moments per Co (black circles) and Fe atoms (blue squares). Shown numbers also include contributions from the small induced moment on W. Red symbols and arrows indicate the clusters that exhibit AFM intra-cluster exchange. Stars are used to denote the moments in tetramers with parallelogram configuration.

Next we tested our results for the different configurations of the initial magnetic moments. In particular, for the rhombic Co_4 system we performed calculations for the different sets of initial moments (ranging from 0 to 5 μ_B, both ferro- and antiferro-magnetic), including non-spin-polarized case. The lowest energy case corresponds to the ferrimagnetic structure reported in the paper. In particular, the non-magnetic state has ~37 meV higher energy that the ferrimagnetic structure. All our calculations are performed for collinear magnetic states.

The calculated energy difference between parallel and antiparallel spin arrangements for the rhombic Co_4 configuration, chosen in the following as a case example, is ΔE = 240 meV. The Heisenberg exchange coupling parameter J_{ij} for nearest Co neighbors, estimated from this value, is 27 meV. The magnitude of the interatomic exchange constants J_{ij} is comparable to that in bulk Co, which is characterized by an interatomic exchange parameter $J_0 = \sum_j J_{0j}$ of 15 meV and a Curie temperature T_C = 1117 °C, but the sign of J_{ij} is negative (AFM). To determine the thermal stability of the spin structures of the tetramers, we have performed Monte Carlo simulations using the Metropolis scheme. The simulations show that the intra-cluster spin correlations are very stable in fields up to 10 T and at temperatures below 100 K.

Figure 2 shows densities of states (DOS) per Co atom for the ferrimagnetic rhombic Co_4 clusters on W(110) and compares the corresponding effective exchange parameter with

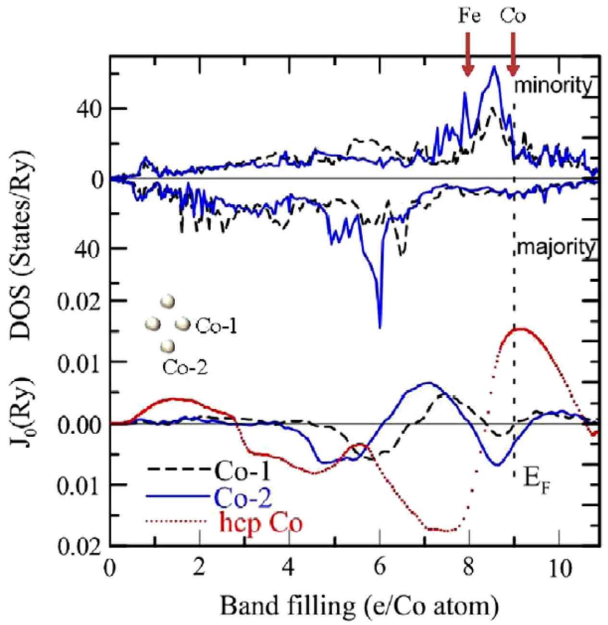

Figure 2. Densities of states and exchange parameter for rhombic clusters: Co DOS for ferrimagnetic Co_4 cluster (top) and calculated exchange parameter J_0 (bottom) as a function of valence band filling for *hcp* Co (dotted red line) and for Co_4/W(110) (solid blue and dashed black lines).

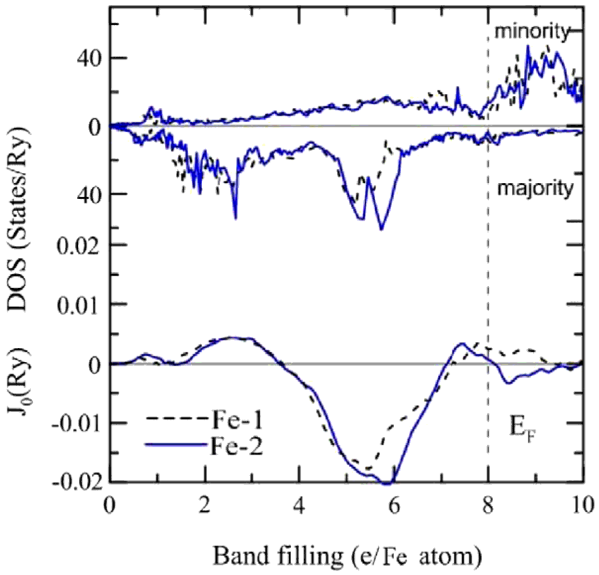

Figure 3. Densities of states and exchange parameter for rhombic clusters: Fe DOS for ferromagnetic cluster (top) and calculated exchange parameter J_0 (bottom) as a function of valence band filling for Fe_4/W(110). Solid blue and dashed black lines correspond to the Fe-1 and Fe-2 atoms, in the same geometry as indicated for the Co-1 and Co-2 atoms in Figure 2.

that of bulk ferromagnets. To compare different iron-series transition-metal elements, we consider the band-filling dependence of the DOS and of J_0, plotting both quantities as a function of the number n of valence electrons per transition-metal atom. Fe and Co correspond to $n = 8$ and $n = 9$, respectively. The dotted red line in Figure 2 (bottom panel) is the well-known band-filling dependence of the exchange in *hcp* bulk materials. More generally, it is known that J_0 is positive for bulk *hcp* Co and *bcc* Fe (ferromagnetism), small and volume dependent for *fcc* Fe (leading to possible non-collinear or spin-density wave structures), and negative for Mn (antiferromagnetism). The overall shape of the $J_0(n)$ curve changes considerably if calculated for Co clusters on W(110) (solid blue and dashed black line), resulting in a negative J_0, or AFM coupling.

A close examination of the band structure for the ferrimagnetic Co_4 cluster shows that the hybridization of Co states with states of the W substrate mediates and modifies the exchange coupling between the Co atoms. A crucial feature of the small clusters is that each Co atom has W atoms as nearest neighbors but Co atoms only as next-nearest neighbors. This means that some Co states, specifically the 'in-plane' xy and $x^2 - y^2$ orbitals, become strongly hybridized with the W states. Since the tungsten substrate exhibits very little spin polarization, it actually suppresses the magnetic moment of the Co xy and $x^2 - y^2$ orbitals.

There is a simple connection between the shape of the $J_0(n)$ curve and the location of the corresponding peaks in DOS in Figure 2. The site-projected DOS of the Co (top panel) exhibits one narrow and localized peak, formed mostly by majority-spin states of xz, yz, and $z^2 - r^2$ character, and a similar peak exists in the minority band. As a result, the exchange coupling exhibits two Fano-like oscillations as a function of band filling, and the Fermi energy of Co_4/W(110), corresponding to $n = 9$, is located in a region where J_0 is negative.

Fe clusters on the other hand have ferromagnetic exchange coupling with the energy of FM state lower than the one of AFM in Fe_4 rhombic cluster by 600 meV. Local magnetic moments of Fe are much larger than in Co_4 cluster (M(Fe-1) = 2.42 μ_B, M(Fe-2) = 2.48 μ_B), and a noticeable magnetization is induced in W substrate (M =− 0.27 μ_B). The local magnetic moments of ferrimagnetic cluster are −1.8 μ_B and 2.2 μ_B, respectively, i.e. reduced with respect to ferromagnetic case. Overall the shape of the $J_0(n)$ as a function of the band filling is similar to the case of Co. With the Fe electron occupancy being smaller than that of Co, the exchange coupling shifts to ferromagnetic as shown in Figure 3. Following the trend we calculated the ground state properties for Mn_4 cluster and found that the exchange is ferromagnetic confirming the extrapolation from $J_0(n)$ calculated the Co_4 cluster calculations. The energy of FM ground state for Mn_4 cluster is lower than that of the ferrimagnetic state by ΔE = 440 meV. Magnetization of the FM Mn_4 cluster is 11.2 μ_B, while in the AFM state the local magnetic moment is reduced only slightly to −2.3 μ_B and +2.7 μ_B, respectively.

In conclusion, our calculations show that atomic clusters of Co on W exhibit magnetic behavior different than other Co systems. In particular, the Co clusters are ferri-, ferro- or non-magnetic, depending on cluster size and geometry. Given the scientific and technological importance of magnetic moment and magnetization, this is a step towards creating unprecedented magnetic materials with interesting new and potentially useful properties. We find surprising trend in the exchange coupling of ultra-small clusters

where Co clusters exhibit ferrimagnetic order (usually not observed in the bulk), while Fe and Mn systems exhibit ferromagnetic order.

Acknowledgments — This work has been supported by the NSF grants DMR-0747704 (CAREER), DMR-0820521 (MRSEC), as well as NRF-20120001875 and NCMN.

References

[1] Kirilyuk A, Giergiel J, Shen J, Straub M, and Kirschner J 1996 *Phys. Rev. B* **54:** 1050
[2] Shen J, Klaua M, Ohresser P, Jenniches H, Barthel J, Mohan Ch V, and Kirschner J 1997 *Phys. Rev. B* **56:** 11134
[3] Kubetzka A, Ferriani P, Bode M, Heinze S, Bihlmayer G, von Bergmann K, Pietzsch O, Blügel S, and Wiesendanger R 2005 *Phys. Rev. Lett.* **94:** 087204
[4] Cort G, Taylor R and Willis J 1982 *J. Appl. Phys.* **53:** 2064
[5] Bode M, Heide M, von Bergmann K, Ferriani P, Heinze S, Bihlmayer G, Kubetzka A, Pietzsch O, Blügel S, and Wiesendanger R 2007 *Nature* **447:** 190
[6] Mohn P and Wohlfarth E P 1987 *J. Phys. F: Met. Phys.* **17:** 2421
[7] Sabiryanov R F, Bose S K, and Mryasov O N 1995 *Phys. Rev. B* **51:** 8958
[8] Bruno P and Sandratskii L 2005 *Phys. J.* **4:** 21
[9] Skomski R and Coey J M D 1999 *Permanent Magnetism* (Bristol: IOP Publishing)
[10] Gambardella P *et al* 2003 *Science* **300:** 1130
[11] Billas I, Chatelain A, and de Heer W A 1994 *Science* **265:** 1682
[12] Guirado-López R, Dorantes-Dávila J, and Pastor G 2003 *Phys. Rev. Lett.* **90:** 226402
[13] Liebermann L, Clinton J, Edwards D, and Mathon J 1970 *Phys. Rev. Lett.* **25:** 232
[14] von Bergmann K, Heinze S, Bode M, Vedmedenko E Y, Bihlmayer G, Blügel S, and Wiesendanger R 2006 *Phys. Rev. Lett.* **96:** 167203
[15] Jamneala T, Madhavan V, and Crommie M F 2001 *Phys. Rev. Lett.* **87:** 256804
[16] Bozorth R M 1951 *Ferromagnetism* (Princeton, NJ: Van Nostrand-Reinhold)
[17] Ferriani P, Heinze S, Bihlmayer G, and Blügel S 2005 *Phys. Rev. B* **72:** 024452
[18] Spišak D and Hafner J 2004 *Phys. Rev. B* **70:** 014430
[19] Garreau G, Farle M, Beaurepaire E, and Baberschke K 1997 *Phys. Rev. B* **55:** 330
[20] Wulfhekel W, Gutjahr-Löser T, Zavaliche F, Sander D, and Kirschner J 2001 *Phys. Rev. B* **64:** 144422
[21] Pinkvos H, Poppa H, Bauer E, and Hurst J 1992 *Ultramicroscopy* **47:** 339
[22] Blöchl P E 1994 *Phys. Rev. B* **50:** 17953
[23] Kresse G and Joubert D 1999 *Phys. Rev. B* **59:** 1758
[24] Perdew J P, Burke K, and Ernzerhof M 1996 *Phys. Rev. Lett.* **77:** 3865
[25] Blöchl P E, Jepsen O, and Andersen O K 1994 *Phys. Rev. B* **49:** 16223
[26] Liechtenstein A I, Katsnelson M I, Antropov V P, and Gubanov V A 1987 *J. Magn. Magn. Mater.* **67:** 65